JOURNAL OF ENVIRONMENTAL SCIENCES 132 (2023) 43–55

Available online at www.sciencedirect.com

ScienceDirect

www.elsevier.com/locate/jes

JES JOURNAL OF ENVIRONMENTAL SCIENCES

www.jesc.ac.cn

Research Article

Parameterization of below-cloud scavenging for polydisperse fine mode aerosols as a function of rain intensity

Chang Hoon Jung[1,*], *Hyung-Min Lee*[2], *Dasom Park*[3], *Young Jun Yoon*[4], *Yongjoo Choi*[5], *Junshik Um*[6], *Seoung Soo Lee*[7,8], *Ji Yi Lee*[2], *Yong Pyo Kim*[9]

[1] *Department of Health Management, Kyungin Women's University, Incheon 21041, Republic of Korea*
[2] *Department of Environmental Science and Engineering, Ewha Woman's University, Seoul, Republic of Korea*
[3] *Department of Environmental Engineering, Konkuk University, Seoul, Republic of Korea*
[4] *Korea Polar Research Institute, Incheon, Republic of Korea*
[5] *Department of Environment, Hankuk University of Foreign Studies, Yongin, Republic of Korea*
[6] *Department of Atmospheric Sciences, Pusan National University, Busan, Republic of Korea*
[7] *Earth System Science Interdisciplinary Center, University of Maryland, College Park, MD, USA*
[8] *Research Center for Climate Sciences, Pusan National University, Busan, Republic of Korea*
[9] *Department of Chemical Engineering and Materials Science, Ewha Womans University, Seoul, Republic of Korea*

ARTICLE INFO

Article history:
Received 16 January 2022
Revised 16 July 2022
Accepted 21 July 2022
Available online 28 July 2022

Keywords:
Below-cloud scavenging
Polydisperse aerosol
Parameterization
Cunningham correction factor
Scavenging coefficient

ABSTRACT

The below-cloud aerosol scavenging process by precipitation is one of the most important mechanisms to remove aerosols from the atmosphere. Due to its complexity and dependence on both aerosol and raindrop sizes, wet scavenging process has been poorly treated, especially during the removal of fine particles. This makes the numerical simulation of below-cloud scavenging in large-scale aerosol models unrealistic. To consider the slip effects of submicron particles, a simplified expression for the diffusion scavenging was developed by approximating the Cunningham slip correction factor. The derived analytic solution was parameterized as a simple power function of rain intensity under the assumption of the lognormal size distribution of particles. The resultant approximated expression was compared to the observed data and the results of previous studies including a 3D atmospheric chemical transport model simulation. Compared with the default GEOS-Chem coefficient of $0.00106R^{0.61}$ and the observation-based coefficient of $0.0144R^{0.9268}$, the coefficient of a and b in $\Lambda_m = aR^b$ spread in the range of 0.0002- 0.1959 for a and 0.3261- 0.525 for b over a size distribution of GSD of 1.3–2.5 and a geometric mean diameter of 0.01- 2.5 µm. Overall, this study showed that the scavenging coefficient varies widely by orders of magnitude according to the size distribution of particles and rain intensity. This study also demonstrated that the obtained simplified expression could consider the theoretical approach of aerosol polydispersity. Our proposed analytic approach showed that results can be effectively applied for reduced computational burden in atmospheric modeling.

Introduction

Aerosols can be removed extensively during the wet deposition process (Jung et al., 2002), which is divided into in-cloud and below-cloud scavenging processes (Textor et al., 2006; Grythe et al., 2017; Choi et al., 2020;). Among these, the below-cloud scavenging process is important to remove coarse and fine particles from the atmosphere (Andronache, 2003).

Typically, the below-cloud scavenging process includes three mechanisms: Brownian diffusion, interception, and impaction (Slinn, 1983). For fine-mode particles with a particle

* Corresponding author.
E-mail: jch@kiwu.ac.kr (C.H. Jung).

https://doi.org/10.1016/j.jes.2022.07.031

size of 0.01–1 µm in diameter, the below-cloud scavenging process is dominated by diffusion and interception mechanisms (Horn et al., 1988; Sparmacher et al., 1993). Generally, the below-cloud scavenging represents a first-order approximation of the particle transfer into raindrops. The governing equation for the wet removal process of particles is expressed as (Prupaccher and Kleet, 1978; Seinfeld and Pandis, 2016):

$$-\frac{\partial n(d_p, t)}{\partial t} = \Lambda(d_p) \cdot n(d_p, t) \tag{1}$$

where, d_p is the diameter of the particle collected, $\Lambda(d_p)$ scavenging coefficient, and $n(d_p,t)$ is the number size distribution of the particles. $\Lambda(d_p)$ is defined as:

$$\Lambda(d_p) = \int_0^\infty K(D_d)E(d_p, D_d)dD_d \tag{2}$$

where, D_d is the diameter of a raindrop collecting, $K(D_d)$ is the collision kernel, and $E(d_p,D_d)$ is the collection efficiency.

Here, the collision kernel is defined as follows:

$$K(D_d) = \frac{\pi D_d^2}{4} U(D_d) n(D_d), \tag{3}$$

where $U(D_d)$ is the fall velocity of a raindrop with diameter D_d and $n(D_d)$ is the number size distribution of raindrops.

One of the most widely used expressions for the scavenging process has been given by Slinn (1983). According to Slinn (1983), the collection efficiency, which considers three particle removal mechanisms (diffusion, interception, and impaction) can be described as follows:

$$E(d_p, D_d) = \frac{4}{ReSc}\left[1 + 0.4Re^{1/2}Sc^{1/3} + 0.16Re^{1/2}Sc^{1/2}\right] + 4\frac{d_p}{D_d}\left[\frac{\mu_a}{\mu_w} + \left(1 + Re^{1/2}\right)\frac{d_p}{D_d}\right] + \left(\frac{St - S^*}{St - S^* + 2/3}\right)^{3/2} \tag{4}$$

where, $Re = \frac{D_d U(D_d)\rho_a}{2\mu_a}$, $Sc = \frac{\mu_a}{\rho_a D_{diff}}$,

$$St = \frac{2\tau U(D_d)}{D_d}, \quad S^* = \frac{1.2 + 1/12\ln(1 + Re)}{1 + \ln(1 + Re)}$$

$$D_{diff} = \frac{k_b T C_c}{3\pi \mu_a d_p}, \quad C_c = 1 + 2.493\frac{\lambda}{d_p} + 0.84\frac{\lambda}{d_p}\exp\left(-0.435\frac{\lambda}{d_p}\right)$$

where, Re is the Reynolds number of a raindrop, Sc is the Schmidt number of the particle, ρ_a (g/cm^3) is the density of the particle, μ_a and μ_w (g/(cm· sec) are the viscosity of air and water drop, respectively, D_{diff} (cm^2/sec) is the vapor diffusivity, C_c is the Cunningham slip correction factor (Gussman, 1969; Hinds, 1998), τ is the relaxation time, k_b (g cm^2/(K·sec^2)) is Boltzmann's constant, λ is the mean free path (cm), and T is the temperature (K). Numerous studies have parameterized the scavenging coefficient as a function of rain intensity (R) (Jylhä, 1991; Laakso et al., 2003; Okita et al., 1996; Wang et al., 2014; Xu et al., 2017; Choi et al., 2020). Here, the collection efficiency is dependent on raindrop and particle sizes. However, there are discrepancies in scavenging coefficients among previous studies, and only few studies have considered the size dependency of the scavenging coefficient (Jung et al., 2002; Bae et al., 2006, Bae et al., 2010).

Over the past few decades, several studies have measured the wet scavenging coefficient using field measurements (Jylhä, 1991; Okita et al., 1996; Laakso et al., 2003; Andronache, 2004; Wang et al., 2014; Xu et al., 2017). These field measurements have used precipitation intensity, cloud-base height, and the ratio between the sulfate concentration in aerosols and rainwater (Okita et al., 1996; Andronache, 2004; Yamagata et al., 2009; Xu et al., 2019).

According to previous studies, washout rates by rain derived from field measurements show differences by a factor of 10 to 100 compared to the values acquired from theoretical calculations (Wang et al., 2010, 2014; Luo et al., 2019). For example, the rain washout rate for water-soluble aerosols measured by Laakso et al. (2003) was 20 times larger than that calculated using semi-empirical parameterizations (Luo et al., 2020). Therefore, Luo et al. (2019) recommended that the empirical scavenging coefficients should be used for simulating washout by rain.

These existing formulae from observations usually do not consider polydisperse size distribution. However, the scavenging coefficient strongly depends on size distribution. This makes the scavenging coefficient-rain intensity parametrization from observation results case-dependent.

Jung et al. (2002) derived analytic solutions for polydisperse particle dynamics using a wet removal process through a theoretical approach. Jung et al. (2003) also developed an expression for the scavenging coefficient as a function of the collection efficiency, the terminal velocity of raindrops, and raindrop and particle size distributions. However, the parameters of the raindrop size distribution used by Jung et al. (2002, 2003) were not sensitive to changes in the rain type or the rain intensity. Bae et al. (2006) developed expressions of the scavenging coefficient for polydisperse aerosols by considering the rain intensity using the moment approach under the assumption of lognormal rain and aerosol size distributions. These distributions were based on the collection efficiency developed by Slinn (1983). Although Bae et al. (2006) considered the polydisperse rain and aerosol size distributions, the expression was too complex for practical applications, especially when the Cunningham correction factor was required for a small-sized regime wherein the particle size was less than 0.1 µm in diameter. Moreover, the lognormal rain distribution assumption is not widely applied compared to the widely used raindrop size distributions, such as the Marshall–Palmer (M–P) raindrop size distribution.

Although many scavenging-related studies exist, physical mechanisms that control the scavenging process have not been clearly understood. Additionally, its parameterization is challenging because the corresponding mechanisms are complex owing to their dependence on aerosol and raindrop size distributions, especially for fine particles. Theoretically, the raindrop diameter should be size-resolved to better simulate real settings. Therefore, a more simplified expression for the scavenging coefficient, which can consider polydisperse rain and aerosol size distributions, is required.

The other issue for simulation of the scavenging process is to reduce the computation burden. The other removal process, such as dry deposition, is computed only for particles very near the ground. However, wet deposition is computed at all heights (Loosmore, et al., 2004).

This computational issue becomes more serious when considering polydisperse aerosols and drop size distribution.

In this study, we try to obtain new analytic expression for scavenging coefficients and collection efficiency for diffusion and interception dominant region that is more simple and can reduce the computational burden in simulating polydisperse aerosol size distribution as well as polydispersed raindrop size distribution than previous studies. We compared our theoretically derived expression (size resolved scavenging coefficient-rain intensity relation) with the existing observation-based expression. Finally, 3D model simulation results were analyzed using these obtained expressions.

Table 1 – Comparison of the C_c expressions.

Reference	Cc expression
Hinds(1998)	$1+2.493\frac{\lambda}{d_p}+0.84\frac{\lambda}{d_p}\exp(-0.435\frac{\lambda}{d_p})$
Hinds(1998)	$1+3.34\frac{\lambda}{d_p}$
Lee and Liu (1980)	1, for large particles with a continuum-flow-regime assumption ($\frac{d_p}{\lambda}\ll 1$); $3.34\frac{\lambda}{d_p}$, for very small particles ($\frac{d_p}{\lambda}\gg 1$); $3.69(\frac{d_p}{\lambda})^{1/2}$, for particles with intermediate sizes.
Jung et al. (2020), This study	$C_c^{2/3}=\{0.6(\frac{d_p}{\lambda})^{0.1}\}^{2/3}\{1+\frac{2}{3}(3.34\frac{\lambda}{d_p})\}$

1. Parameterization of the below-cloud scavenging coefficient

1.1. *Analytic expression for below-cloud scavenging coefficient for polydisperse aerosols*

1.1.1. *Collection efficiency and approximation of Cunningham slip correction factor*

The scavenging coefficient Eq. (2) can be obtained by multiplying collection efficiency (Eq. (4)), collision kernel (Eq. (3)) and integrating over particle diameter. As a formula described in Eq. (4), integration on Eq. (2) cannot be obtained analytically. The main reason for the difficulty in obtaining analytic expression is the complex formula of Cunningham slip correction factor (C_c).

By introducing collection efficiency based on the simple expression (Jung et al., 2002) and adapting the approximation of C_c, we can obtain an analytic expression of the scavenging coefficient for polydisperse aerosol size distribution.

The collection efficiency in the diffusion (E_D) and interception regions (E_R) can be expressed as follows (Jung et al., 2002):

$$E_D(d_p,D_d)=2\left(\frac{\sqrt{3}\pi}{4Pe}\right)^{2/3}\left[\frac{(1-\alpha)(3\sigma+4)}{J+\sigma K}\right]^{1/3} \tag{5}$$

$$E_R(d_p,D_d)=\left[\frac{(1-\alpha)}{(J+\sigma K)}\right]d_pD_d^{-1}+\left[\frac{(1-\alpha)(3\sigma+4)}{2(J+\sigma K)}\right]d_p^2D_d^{-2} \tag{6}$$

where, $Pe=\frac{D_dU(D_d)}{D_{diff}}$, σ is the viscosity ratio of water to air, $J=1-\frac{6}{5}\alpha^{\frac{1}{3}}+\frac{1}{5}\alpha^2$, $K=1-\frac{9}{5}\alpha^{\frac{1}{3}}+\alpha+\frac{1}{5}\alpha^2$, and α and Pe are the packing density and Peclet number, respectively. By using packing density, the effects of flow due to neighboring droplets can be considered (Lee et al., 1978; Jung and Lee, 1998; Ardon-Dryer et al., 2015). In this study, we assume the packing density (α) to be 0 under the assumption that the flow of raindrops is not affected by neighboring droplets. However, this neighboring collector effect can be usefully applied to concentric collector systems such as a granular filter or heavy precipitation (Lee et al., 1978; Jung et al., 2000). The collection efficiency due to diffusion increases as the particle diameter decreases. Moreover, the collection efficiency due to interception increases as the particle diameter increases.

Here, for the diffusion region in Eq. (5), Pe and a related variable D_{diff} can be expressed as a function of C_c, which is closely linked to the aerosol diameter. Because of the complexity in the expression of Pe and $E_D(d_p,D_d)$ with the consideration of polydispersity in C_c, a simple and accurate expression to describe the scavenging coefficient in the diffusion dominant region is required, which has been explained in detail in Appendix. Thus, in this study, a simplified expression for the scavenging coefficient in the diffusion region was developed by adopting C_c approximation and the M–P raindrop size distribution.

When the size of aerosol particles in a medium approaches the mean free path of gas molecules, discontinuities in the medium should be considered, The Cunningham correction factor explains these discontinuities (Gussman, 1969; Hinds, 1998). Many studies have been carried out to characterize the slip correction factor as a function of the Knudsen number. Several experimental investigations were performed to obtain empirical equations of the slip correction factor for a wide range of Knudsen numbers. Table 1 shows the comparison of the C_c expressions.

The general form of C_c can be expressed as follows (Hinds, 1998):

$$C_c=1+2.493\frac{\lambda}{d_p}+0.84\frac{\lambda}{d_p}\exp\left(-0.435\frac{\lambda}{d_p}\right) \tag{7}$$

However, this expression is complex and requires simplification for parameterization studies (Hinds, 1998; Sorensen and Wang, 2000; Jung et al., 2020). Many studies have showed a variety of C_c expressions (Lee and Liu, 1980; Allen and Raabe, 1985; Hinds, 1998; Schmid et al., 2002; Jung et al., 2020).

One of the simplified expressions for C_c that is frequently used in many studies is as follows (Lee and Liu, 1980; Hinds, 1998):

$$C_c\cong 1+3.34\frac{\lambda}{d_p}, \tag{8}$$

This simplified expression for C_c is accurate enough compared to the original expression (Lee and Liu, 1980). However, to integrate C_c over polydispersed aerosol size distribution using the moment formula under the assumption of a log-normal size distribution, a more simplified expression is required (Jung et al., 2020). Lee and Liu (1980) approximated the C_c for three different size ranges, as shown in Table 1. Although these approximations showed good correlations with the original equation make it possible to integrate collection efficiency and scavenging coefficient over polydisperse size distribution, the approximated equations are valid only for the given size conditions and require different approximations in other size ranges. Additionally, the original and simplified C_c from previous studies (Lee and Liu, 1980; Hinds, 1998) have limitations in representing the collection efficiency due to diffusion and the scavenging coefficient for polydisperse aerosol analytically.

In this study, to address these limitations, we used a more simplified expression for the slip correction efficiency, which can cover all size ranges as one expression (Jung et al., 2020).

$$C_c = \left\{0.6\left(\frac{d_p}{\lambda}\right)^{0.1}\right\}\left\{1+\frac{2}{3}\left(3.34\frac{\lambda}{d_p}\right)\right\}^{3/2} \tag{9}$$

By applying Eq. (9) to Eq. (5), the subsequent collection efficiency due to diffusion can be expressed as a linear polynomial equation of the particle diameter (d_p).

$$E_D(d_p, D_d) = \left(\xi_1 d_p^{-3/5} + \xi_2 d_p^{-8/5}\right) D_d^{-2/3} \tag{10}$$

where,

$$\xi_1 = 2\left(\frac{\sqrt{3}\pi}{4}\right)^{2/3}\left[\frac{(1-\alpha)(3\sigma+4)}{J+\sigma K}\right]^{1/3} 0.6^{2/3}\left(\frac{1}{\lambda}\right)^{1/15}\left(\frac{kT}{3\pi\mu U(D_d)}\right)^{2/3}$$

$$\xi_2 = 2\left(\frac{\sqrt{3}\pi}{4}\right)^{2/3}\left\{\frac{2}{3}(3.34\lambda)\right\}\left[\frac{(1-\alpha)(3\sigma+4)}{J+\sigma K}\right]^{1/3} 0.6^{2/3}\left(\frac{1}{\lambda}\right)^{1/15}\left(\frac{kT}{3\pi\mu U(D_d)}\right)^{2/3}$$

For interception, the collection efficiency can be described as:

$$E_R(d_p, D_d) = \xi_3 d_p D_d^{-1} + \xi_4 d_p^2 D_d^{-2} \tag{11}$$

where $\xi_3 = [\frac{(1-\alpha)}{(J+\sigma K)}]$,

$$\xi_4 = \left[\frac{(1-\alpha)(3\sigma+4)}{2(J+\sigma K)}\right]$$

One of the important factors that affect the scavenging of aerosols by rain is its fall velocity. The general expression for the fall velocity is a power law type function of the drop diameter (D_d) (Jung et al., 2002):

$$U(D_d) = \gamma D_d^{\beta}, \tag{12}$$

where γ and β are constants.

By applying Eq. (10), the resultant collection efficiency can be rewritten as follows:

$$E_D(d_p, D_d) = \left(\xi'_1 d_p^{-3/5} + \xi'_2 d_p^{-8/5}\right) D_d^{-\frac{2}{3}(1+\beta)} \tag{13}$$

where

$$\xi'_1 = 2\left(\frac{\sqrt{3}\pi}{4}\right)^{2/3}\left[\frac{(1-\alpha)(3\sigma+4)}{J+\sigma K}\right]^{1/3} 0.6^{2/3}\left(\frac{1}{\lambda}\right)^{1/15}\left(\frac{kT}{3\pi\mu\gamma}\right)^{2/3}$$

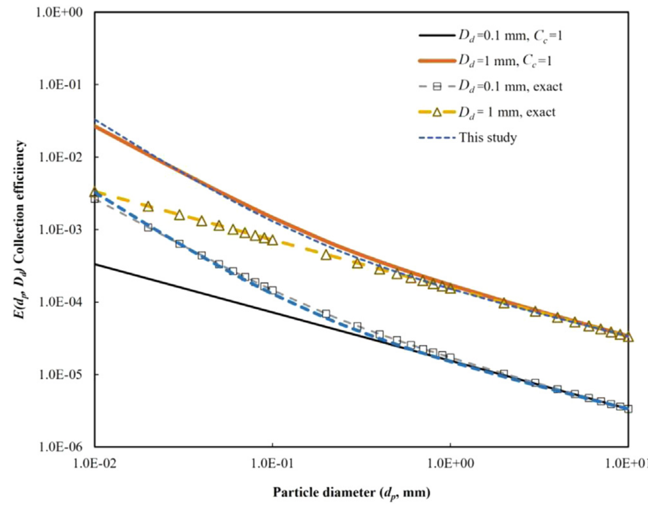

Fig. 1 – Comparison of the collections efficiency due to diffusion ($E(d_p, D_d)$) as a function of the particle diameter obtained in this study with the Slinn's collection efficiency (C_c= 1, C_c as an exact solution and approximated C_c from this study).

$$\xi'_2 = 2\left(\frac{\sqrt{3}\pi}{4}\right)^{2/3}\left\{\frac{2}{3}(3.34\lambda)\right\}\left[\frac{(1-\alpha)(3\sigma+4)}{J+\sigma K}\right]^{1/3} 0.6^{2/3}\left(\frac{1}{\lambda}\right)^{1/15}\left(\frac{kT}{3\pi\mu\gamma}\right)^{2/3}$$

Fig. 1 shows the collection efficiency, which is related to diffusion ($E_D(d_p, D_d)$) and a function of the particle diameter for different C_c values. For $C_c = 1$ (neglecting the Cunningham slip effect), the exact solution (Eq. (7)), and the approximated values from this study (Eq. (9)) were compared. Here, the drop diameters (D_d) of each of 0.1 mm and 1 mm were considered.

According to Fig. 1, the approximated collection efficiency in this study showed good agreement with the exact solution. However, the discrepancy between the approximated and the exact solutions increased as the particle diameter decreased. Fig. 2 shows a comparison of the collection efficiency between Slinn's formula as shown in Eq. (4) and this study Eqs. (5) and ((6)). The drop diameters of 0.1 mm and 1 mm were compared. As shown in Fig. 2, both Slinn's formula and this study showed a similar tendency and were comparable to each other. According to Fig. 2, the collection efficiency from Slinn's formula showed a higher value compared to that observed in this study.

1.1.2. *Scavenging coefficient*

From Eqs. (2), (11), (12) and (13), the scavenging coefficient for polydisperse rain and aerosol distribution is given as follows:

$$\begin{aligned}\Lambda(d_p) &= \int_0^\infty \frac{\pi}{4} D_d^2 U(D_d) E(D_d, d_p) n(D_d) dD_d \\ &= \int_0^\infty \frac{\pi}{4} D_d^2 U(D_d)\left\{\left(\xi'_1 d_p^{-3/5} + \xi'_2 d_p^{-8/5}\right) D_d^{-\frac{2}{3}(1+\beta)} + \xi_3 d_p D_d^{-1} + \xi_4 d_p^2 D_d^{-2}\right\} n(D_d) dD_d \\ &= \int_0^\infty \frac{\gamma\pi}{4}\left\{\left(\xi'_1 d_p^{-3/5} + \xi'_2 d_p^{-8/5}\right) D_d^{\frac{1}{3}(\beta+4)} + \xi_3 d_p D_d^{\beta+1} + \xi_4 d_p^2 D_d^{\beta}\right\} n(D_d) dD_d\end{aligned} \tag{14}$$

Despite many raindrop measurement techniques, it is still difficult to directly measure the raindrop size distribution

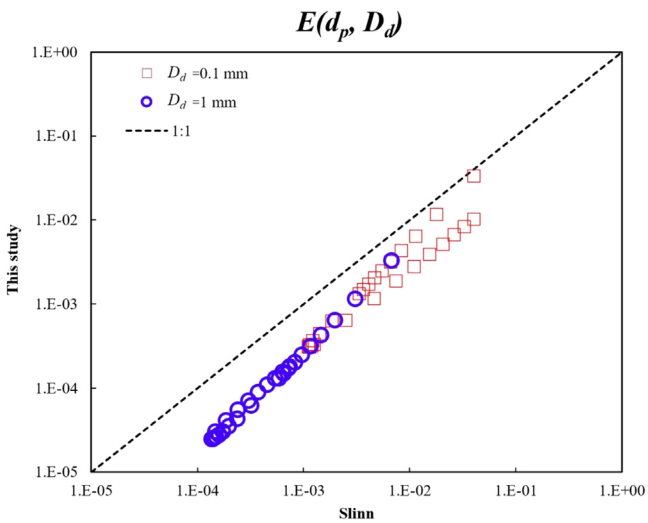

Fig. 2 – Comparison of the collection efficiency in association with diffusion and interception between Slinn's formula in Eq. (4) and this study.

with precision; however, rain intensity can be easily measured (Kathiravelu et al., 2016). Thus, various scavenging coefficients, expressed as constants or functions of the precipitation intensity, are used in regional or mesoscale Lagrangian and Eulerian models to describe the precipitation and the wet removal of pollutants (Bae et al., 2006; Seinfeld and Pandis, 2016).

There are three most widely used raindrop size distributions: Gamma distribution, Marshall-Palmer (M-P) distribution, and log-normal size distribution (; Ekerete et al., 2015). In this study, we considered the M-P drop size distribution. Although the M–P distribution has been proposed several decades ago and have several limitations regarding its accuracy compared with measurement studies, it remains one of the most common and classical raindrop size distributions (Croft et al., 2009; Liu et al., 2018).

The M-P distribution is an exponential size distribution, in which the number concentration decreases exponentially as the drop diameter increases.

The M–P raindrop size distribution can be expressed as (Marshall and Palmer, 1948):

$$n(D_d) = N_0 e^{-4.1\mathrm{R}^{-0.21} D_d} \tag{15}$$

Here, N_0 is the number concentration parameter (8000 $m^{-3}mm^{-1}$) and R is rain intensity (mm/hr).

The scavenging coefficient for the M–P raindrop size distribution can be obtained as follows:

$$\Lambda(d_p) = \int_0^{\infty} \frac{\gamma\pi}{4}\left\{\left(\xi'_1 d_p^{-3/5} + \xi'_2 d_p^{-8/5}\right) D_d^{\frac{1}{3}(\beta+4)} + \xi_3 d_p D_d^{\beta+1} + \xi_4 d_p^2 D_d^{\beta}\right\} N_0 e^{-4.1\mathrm{R}^{-0.21} D_d} dD_d \tag{16}$$

Subsequently, the final scavenging coefficient can be expressed as follows:

$$\Lambda(d_p) = \phi_1(\mathrm{R},\beta) d_p^{-\frac{3}{5}} + \phi_2(\mathrm{R},\beta) d_p^{-\frac{8}{5}} + \phi_3(\mathrm{R},\beta) d_p + \phi_4(\mathrm{R},\beta) d_p^2 \tag{17}$$

where $\phi_1(\mathrm{R},\beta) = \frac{\gamma\pi}{4} N_0 \xi'_1 f_1(\mathrm{R},\beta)$, $\phi_2(\mathrm{R},\beta) = \frac{\gamma\pi}{4} N_0 \xi'_2 f_1(\mathrm{R},\beta)$, $\phi_3(\mathrm{R},\beta) = \frac{\gamma\pi}{4} N_0 \xi_3 f_2(\mathrm{R},\beta)$, and $\phi_4(\mathrm{R},\beta) = \frac{\gamma\pi}{4} N_0 \xi_4 f_3(\mathrm{R},\beta)$.

According to Kessler (1969), the raindrop fall velocity is expressed as $\gamma = 130$ and $\beta = 0.5$. If we follow Kessler's parameterization of the fall velocity of the raindrop, which is proportional to the square root of the drop diameter ($\beta = 0.5$), f_1, f_2, and f_3 can be approximated as the power of rain intensity (R).

$$f_1(\mathrm{R},\beta) = \int_0^{\infty} D_d^{\frac{1}{3}(\beta+4)} e^{-4.1\mathrm{R}^{-0.21} D_d} dD_d \cong 0.0391\mathrm{R}^{0.525}$$

$$f_2(\mathrm{R},\beta) = \int_0^{\infty} D_d^{\beta+1} e^{-4.1\mathrm{R}^{-0.21} D_d} dD_d \cong 0.0387\mathrm{R}^{0.5234}$$

$$f_3(\mathrm{R},\beta) = \int_0^{\infty} D_d^{\beta} e^{-4.1\mathrm{R}^{-0.21} D_d} dD_d \cong 0.1068\mathrm{R}^{0.315} \tag{18}$$

It should be noted that the approach from this study can also consider other raindrop size distribution, such as Gamma and lognormal raindrop size distributions. For example, the Gamma raindrop size distribution can be expressed as below:

$$n(D_d) = N_0 D_d^{\delta} e^{-\Psi D_d} \tag{19}$$

Here, δ is the shape distribution parameter and Ψ is the slope parameter for Gamma raindrop distribution.

The scavenging coefficient for the Gamma raindrop size distribution can be obtained as follows:

$$\Lambda(d_p) = \int_0^{\infty} \frac{\gamma\pi}{4}\left\{\left(\xi'_1 d_p^{-3/5} + \xi'_2 d_p^{-8/5}\right) D_d^{\frac{1}{3}(\beta+4)+\delta} + \xi_3 d_p D_d^{\beta+\delta+1} + \xi_4 d_p^2 D_d^{\beta+\delta}\right\} N_0 e^{-\Psi D_d} dD_d \tag{20}$$

For lognormal raindrop size distribution, Eq. (14) can be expressed as follows:

$$\Lambda(d_p) = \int_0^{\infty} \frac{\gamma\pi}{4}\left\{\left(\xi'_1 d_p^{-3/5} + \xi'_2 d_p^{-8/5}\right) D_d^{\frac{1}{3}(\beta+4)} + \xi_3 d_p D_d^{\beta+1} + \xi_4 d_p^2 D_d^{\beta}\right\} n(D_d) dD_d$$

$$= \left(\xi'_1 d_p^{-3/5} + \xi'_2 d_p^{-8/5}\right) X_{\frac{1}{3}(\beta+4)} + \xi_3 d_p X_{\beta+1} + \xi_4 d_p^2 X_{\beta} \tag{21}$$

where X_k is the kth moment for lognormal raindrop size distribution.

$$X_k = \int_0^{\infty} D_d^k n(D_d) dD_d = X_0 D_g^k exp\left[\frac{k^2}{2} ln^2(GSD_{Drop})\right] \tag{22}$$

where D_g and GSD_{Drop} are the geometric mean diameter and geometric standard deviation of rain drop size distribution, respectively, and X_0 represents the total number of droplets.

Fig. 3 shows the $\Lambda(d_p)$ as a function of the particle diameter and rain intensity. The M–P rain size distribution along with rain intensities of 0.1, 1 , 10 , and 100 mm/hr are considered. As shown in Fig. 3, the scavenging coefficient decreased as the rain intensity decreased. Fig. 3 also shows that the scavenging coefficient decreased as the particle diameter increased because of the diffusion mechanism in the submicron region. For larger-sized regime where the particle diameter was larger than several microns in diameter, the scavenging coefficient increased as the particle diameter increased owing to interception.

For polydisperse aerosols, the resultant governing equation of the wet removal process can be expressed based on Eq. (1) as follows:

$$-\int_0^{\infty} \frac{\partial n(d_p)}{\partial t} dd_p = \int_0^{\infty} \Lambda(d_p, \mathrm{R}) n(d_p) dd_p \tag{23}$$

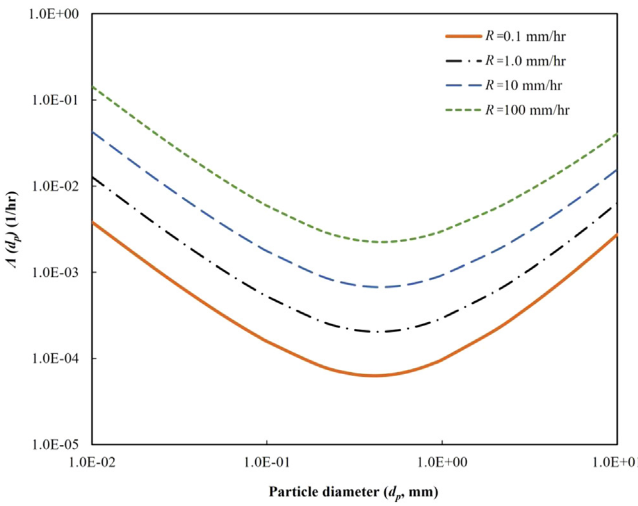

Fig. 3 – Mass scavenging coefficient obtained in this study as a function of particle diameter and rain intensity.

1.1.3. *Scavenging coefficient for polydisperse aerosols*

In this study, the lognormal size distribution was assumed for polydisperse aerosols. By introducing the representation of moment equations for the lognormal distribution, the k$^{\text{th}}$ moment (M_k) can be expressed as (Jung et al., 2002):

$$M_k = \int_0^\infty d_p^k n(d_p) dd_p = M_0 d_g^k exp\left[\frac{k^2}{2} ln^2(GSD)\right] \tag{24}$$

where, d_g and GSD are the geometric mean diameter and geometric standard deviation, respectively. M_0 represents the total number of particles and $(\pi/6)M_3$ is the total volume concentration.

Based on Eqs. (16)–(18) and (23), the subsequent number-mean scavenging coefficient can be described as follows:

$$-\int_0^\infty \frac{\partial n(d_p)}{\partial t} dd_p = \int_0^\infty \Lambda(d_p, R) n(d_p) dd_p$$
$$= \phi_1(R, \beta)M_{-3/5} + \phi_2(R, \beta)M_{-8/5} + \phi_3(R, \beta)M_1 + \phi_4(R, \beta)M_2 \tag{25}$$

The scavenging coefficient is based on the aerosol number size distribution. However, in many observations, the scavenging coefficient has been described based on the mass size distribution.

The mass-mean scavenging coefficient (Λ_m) can be obtained using Eq. (25),

$$-\int_0^\infty \frac{\pi\rho_p}{6} d_p^3 \frac{\partial n(d_p)}{\partial t} dd_p = \int_0^\infty \frac{\pi\rho_p}{6} d_p^3 \Lambda(d_p, R) n(d_p) dd_p =$$
$$\frac{\frac{\pi\rho_p}{6}[\phi_1(R, \beta)M_{3-3/5} + \phi_2(R, \beta)M_{3-8/5} + \phi_3(R, \beta)M_{3+1} + \phi_4(R, \beta)M_{3+2}]}{\int_0^\infty \frac{\pi\rho_p}{6} d_p^3 n(d_p) dd_p}$$
$$\int_0^\infty \frac{\pi\rho_p}{6} d_p^3 n(d_p) dd_p. \tag{26}$$

The resultant expression can be expressed as

$$-\frac{\partial C}{\partial t} = \frac{\left[\phi_1(R, \beta)M_{\frac{12}{5}} + \phi_2(R, \beta)M_{\frac{7}{5}} + \phi_3(R, \beta)M_4 + \phi_4(R, \beta)M_5\right]}{M_3} C = \Lambda_m C \tag{27}$$

Here,

$$\Lambda_m = \frac{\left[\phi_1(R, \beta)M_{\frac{12}{5}} + \phi_2(R, \beta)M_{\frac{7}{5}} + \phi_3(R, \beta)M_4 + \phi_4(R, \beta)M_5\right]}{M_3}. \tag{28}$$

For multimodal aerosol, the scavenging coefficient can be expressed as follows:

$$-\frac{\partial C}{\partial t} = -\sum_i \frac{\partial C_i}{\partial t} = \sum_i \Lambda_{m,i} C_i. \tag{29}$$

where

$$\Lambda_{m,i} = \frac{\left[\phi_1(R, \beta)M_{\frac{12}{5},i} + \phi_2(R, \beta)M_{\frac{7}{5},i} + \phi_3(R, \beta)M_{4,i} + \phi_4(R, \beta)M_{5,i}\right]}{M_{3,i}}. \tag{30}$$

The moment expression M_k in Eq. (24) is based on the number size distribution (Jung et al., 2002; Bae et al., 2006). The d_g in Eq. (24) is the number-mean geometric mean diameter. The relation between the geometric volume-mean (d_{gv}) and number-mean (d_g) diameter can be expressed as follows:

$$d_{gv} = d_g exp\left[3ln^2(GSD)\right] \tag{31}$$

1.2. *Newly derived scavenging coefficient-rain intensity parameterization for polydisperse aerosol*

The resultant mass scavenging coefficient in Eq. (27), was a function of d_g, GSD, and rain intensity, and it could be parameterized to a greater degree that could enhance the applicability of the coefficient in measurement and model studies.

The conventional expression for the aerosol-scavenging coefficient can be expressed as a power of rain intensity.

$$\Lambda_m = a \times R^b \tag{32}$$

The resultant Eq. (32) was simplified as a function of the conventional scavenging parameterization in the form of the power of rain intensity.

Based on the theoretical expressions in Eqs. (27)-(30), the coefficients a and b in Eq. (32) could be estimated by the regression of the polydisperse aerosol size distribution.

For the polydisperse aerosol size distribution in the range of 0.01–1 µm with a geometric standard deviation of 1.3–2.5, the resultant coefficients a and b could be approximated as a function of d_g (in µm) and GSD and parameterized as follows:

$$a = a_{11} d_g^{-a_{12}} + a_{21} d_g^{a_{22}}$$

$$b = b_{11} d_g^{-b_{12}} \tag{33}$$

where,

$$a_{11} = -1.5 \times 10^{-5} GSD + 4.1 \times 10^{-5},\ a_{12} = -0.042 GSD + 1.2447,$$

$$a_{21} = 2 \times 10^{-5} GSD^{8.1029},\ a_{22} = 0.9776 GSD^{0.5774},$$

$$b_{11} = -0.1321 GSD + 0.6755 b_{12} = 0.073 GSD - 0.079.$$

Table 2 – Size resolved below-cloud scavenging coefficient parameters *a* and *b* ($\Lambda_m = aR^b$, h^{-1}) estimated based on Eq. (33) in the text.

(a) *a* values

$\sigma_g d_g$	1.3	1.5	1.7	1.9	2.1	2.3	2.5
0.01	0.0101	0.0074	0.005	0.0032	0.0021	0.0013	0.0009
0.03	0.002	0.0015	0.001	0.0007	0.0005	0.0004	0.0003
0.05	0.001	0.0008	0.0006	0.0004	0.0003	0.0003	0.0004
0.07	0.0007	0.0005	0.0004	0.0003	0.0003	0.0003	0.0005
0.1	0.0004	0.0004	0.0003	0.0003	0.0003	0.0004	0.0007
0.2	0.0002	0.0002	0.0002	0.0003	0.0004	0.0008	0.0019
0.3	0.0002	0.0002	0.0002	0.0004	0.0006	0.0014	0.0037
0.4	0.0002	0.0002	0.0003	0.0005	0.001	0.0023	0.0061
0.5	0.0002	0.0002	0.0004	0.0006	0.0013	0.0033	0.0091
0.6	0.0002	0.0003	0.0004	0.0008	0.0018	0.0045	0.0127
0.7	0.0002	0.0003	0.0005	0.001	0.0023	0.0059	0.0169
0.8	0.0003	0.0004	0.0006	0.0012	0.0028	0.0075	0.0217
0.9	0.0003	0.0004	0.0007	0.0014	0.0034	0.0093	0.0272
1	0.0003	0.0005	0.0008	0.0017	0.0041	0.0112	0.0332
1.5	0.0005	0.0008	0.0015	0.0033	0.0084	0.0239	0.0724
2	0.0007	0.0011	0.0023	0.0053	0.0142	0.0412	0.1266
2.5	0.0009	0.0016	0.0033	0.0079	0.0214	0.0632	0.1959

(b) *b* values

$\sigma_g d_g$	1.3	1.5	1.7	1.9	2.1	2.3	2.5
0.01	0.525	0.525	0.525	0.525	0.525	0.5249	0.5244
0.03	0.525	0.525	0.5249	0.5248	0.524	0.5211	0.5111
0.05	0.525	0.5249	0.5247	0.5239	0.5209	0.5113	0.4881
0.07	0.5249	0.5247	0.5242	0.5222	0.5157	0.4987	0.4674
0.1	0.5247	0.5243	0.5228	0.5182	0.5057	0.4804	0.4441
0.2	0.523	0.5206	0.514	0.4993	0.4736	0.4389	0.4022
0.3	0.5199	0.5146	0.5028	0.4815	0.4507	0.4151	0.3816
0.4	0.5158	0.5078	0.4921	0.467	0.4342	0.3993	0.369
0.5	0.5114	0.5011	0.4825	0.455	0.4215	0.388	0.3605
0.6	0.5068	0.4947	0.474	0.445	0.4114	0.3795	0.3532
0.7	0.5024	0.4887	0.4664	0.4365	0.4032	0.3727	0.3496
0.8	0.4981	0.4831	0.4596	0.4291	0.3963	0.3673	0.3459
0.9	0.494	0.478	0.4535	0.4226	0.3904	0.3628	0.343
1	0.4901	0.4732	0.4479	0.4168	0.3853	0.3591	0.3405
1.5	0.4732	0.4533	0.426	0.3956	0.3678	0.3466	0.3328
2	0.4597	0.4383	0.4107	0.3819	0.3573	0.3397	0.3286
2.5	0.4486	0.4264	0.3991	0.3722	0.3503	0.3353	0.3261

Fig. A1 shows a_{11}, a_{12}, b_{11}, and b_{12} for the parameterization of *a* and *b* in Eq. (33).

The resultant parameters in Eq. (33) could describe Λ_m as a function of the geometric standard deviation and geometric mean diameter with a simplified expression. Table 2 shows the size resolved below-cloud scavenging coefficient parameters *a* and *b* ($\Lambda_m = aR^b$, h^{-1}). As Table 2 shows, the analytic estimation showed a value range of 0.0002–0.1959 for 0.01–2.5 µm d_g and 1.3–2.5 of GSD. Coefficient *b* was in the range of 0.3261–0.525. This coefficients spreads over wide ranges with the order of magnitude (in case of *a*), but comparable with the reported coefficients in the previous studies (Okita et al., 1996; Baklanov and Sørensen, 2001; Andronache, 2003) which will be discussed in Table 3. Fig. 4 shows the comparison of the parameters of the scavenging coefficients (*a* and *b*, where $\Lambda_m = aR^b$) for polydisperse size distribution between the regression-derived estimation and the simple approximated parameterization from Eq. (33). As shown in Fig. 4, the parameterized coefficients (*a* and *b*) from Eq. (33) agreed well with the regression-estimated counterparts. The coefficient *a* increased as d_g decreased for the diffusion-dominant regime and d_g increased for the interception dominant region. These tendencies showed different values depending on the GSD. The coefficient *b* decreased as d_g and GSD increased.

The obtained resultant analytic expressions in Eqs. (32) and (33) were parameterized approximations based on the theoretical study. Fig. 5 shows a comparison of the below-cloud scavenging coefficient for the polydisperse size distribution as a function of rain intensity. The mass scavenging efficiencies with different d_g of 0.01 µm, 0.1 µm, and 0.5 µm and GSDs of 1.5, 2.0, and 2.5 were compared. As shown in Fig. 5, the mass scavenging coefficients increased as the rain intensity increased and this increase in the coefficient depended on the size distribution. For $d_g = 0.01$ µm, the mass scavenging coefficient increased as d_g decreased. When GSD = 1.5, the mass scavenging coefficient increased as d_g decreased. For example, the scavenging coefficient increased as the particle

Table 3 – Below-cloud scavenging coefficient (Λ_m, hr^{-1}) expressed as aR^b (where the rainfall rate R is in mm/hr).

A	b	Reference	Note
0.36	0.67–0.76	Okita et al. (1996)	Experimental estimation for total wet scavenging by Okita et al. (1996)
0.24	0.7	Andronache (2003)	Urban. Cases with coarse mode. Calculations are based on the aerosol types by Jaenicke (1993)
0.07308	0.543	Choi et al. (2020)	
1.26	0.78	Scott (1982)	Model calculated in-cloud scavenging coefficient for aerosol particles grown at the size of cloud droplet with dp = 10 µm particle
0.9	0.61	Xu et al. (2017)	NO_3^-, Field measurement (Beijing, China)
0.2736	0.8	Xu et al. (2017)	SO_4^{2-}, Field measurement (Beijing, China)
0.396	0.52	Xu et al. (2017)	NH_4^+, Field measurement (Beijing, China)
0.025	0.92	Jylhä (1999)	Model calculated values for particles with diameters in the range [0.3–0.9] µm and assumed $E = 0.02$
0.3024	0.79	Baklanov and Sørensen (2001)	Theoretical calculation (d_p <1.4µm)
0.00106	0.61		GEOS-Chem Fine mode
1.57	0.79		GEOS-Chem Coarse mode
0.0144	0.9268		This study (from PM_{10} observation)
0.0074	0.525	This Study (Analytic)	d_{g0}=0.01 µm, GSD=1.5
0.0002	0.5011		d_{g0}=0.5 µm, GSD=1.5
0.0016	0.4264		d_{g0}=2.5 µm, GSD=1.5
0.0009	0.5244		d_{g0}=0.01 µm, GSD=2.5
0.0091	0.3605		d_{g0}=0.5 µm, GSD=2.5
0.1959	0.3261		d_{g0}=2.5 µm, GSD=2.5

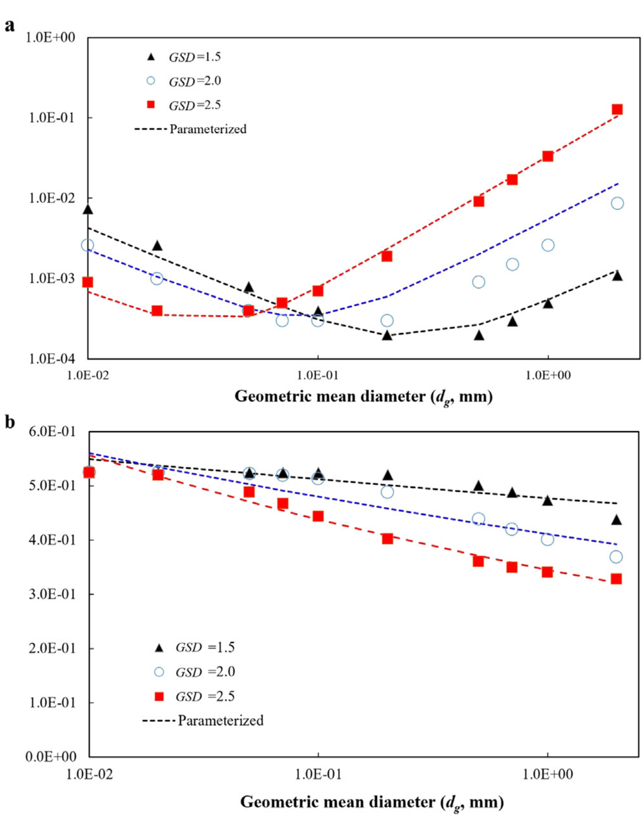

Fig. 4 – Parameters of scavenging coefficients (*a* and *b*, where $\Lambda_m = aR^b$) for polydisperse size distribution.

diameter decreased in the diffusion-dominant regime. However, the scavenging coefficient increased as the particle diameter increased for the interception and impaction dominant regimes.

2. Observation-based scavenging coefficient and 3D model simulation

In this study, we compared our result with the previous experimental and theoretical studies. We also compared our results with the observation.

If it is assumed that the scavenging coefficient is constant with respect to time, the equation of the scavenging coefficient is defined as follows (Sperber andHameed, 1986; Laakso et al., 2003).

$$\Lambda_m = \frac{1}{t} ln\left(\frac{C_t}{C_0}\right) \quad (34)$$

where C_0 and C_t are the mass concentration of the particles before (C_0) and after (C_t) the precipitation starts, and t is a time when the precipitation starts. In this study, scavenging coefficients were calculated based on measurements from 5 major cities (Seoul, Pusan, Gwangju, Daejeon, Daegu), in Korea. From January to March 2019, hourly PM_{10} observations from each air pollution monitoring station were matched with nearby weather monitoring stations in the cities of Korea, only if the distance between an air pollution station and the nearest weather stations was less than 7.5 km.

A total of 52 precipitation cases were observed at five weather stations, and their precipitation intensity ranged from 0.086 to 4 mm/hr, as shown in Fig. A2. The probabil-

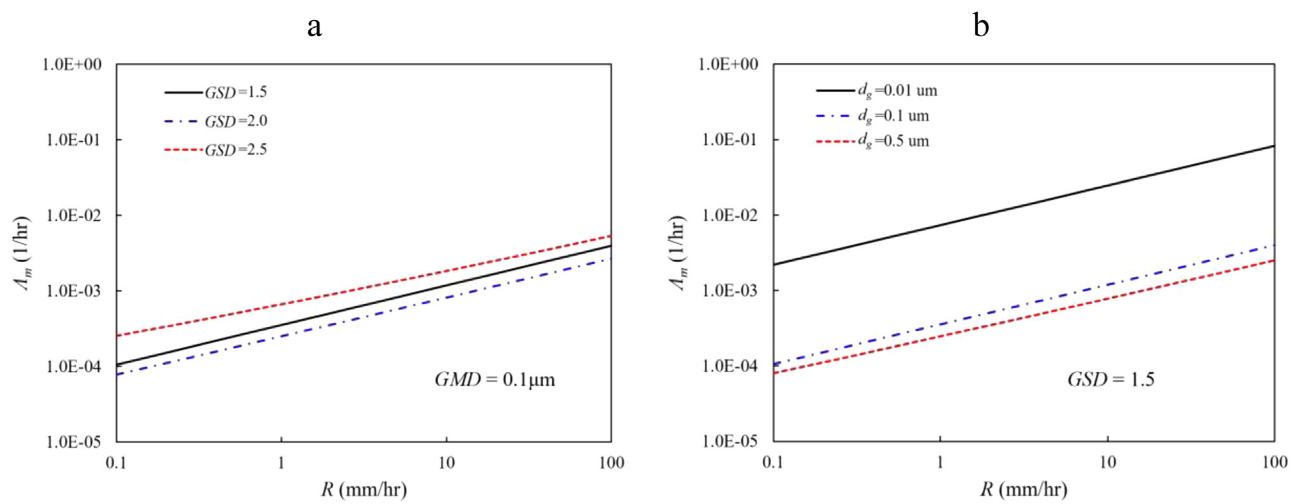

Fig. 5 – Comparison of the mass scavenging coefficient as a function of rain intensity with different geometric standard deviations and geometric mean diameters.

ity density function graph of precipitation intensity shows a right-skewed distribution. Winter was partially included in the period; thus, there was relatively less precipitation owing to the characteristics of precipitation in Korea. Thus, weak intensity precipitation cases were measured frequently. For all rainfall cases, the scavenging coefficient was calculated using Eq. (34) and related to the rainfall intensity at the time. In this study, the median of the scavenging coefficients was used because the median of the scavenging coefficients had less variation and was less sensitive to possible sudden changes in air masses, comparing with mean as an ensemble mean statistic for scavenging coefficients (Laakso et al., 2003). As shown in the results of Table A1, rainfall intensity was divided into four bins to calculate the median value of each bin.

Based on the measurement data, the resultant median scavenging coefficients (Λ_m, hr^{-1}) can be expressed as a function of the rain intensity:

$$\Lambda_m = 0.0144R^{0.9268} \tag{35}$$

Fig. 6 shows an observation-based scavenging coefficient as a rain intensity. The scavenging coefficient between current study and Laakso et al.(2003) was compared. The scavenging efficiency calculated in Fig. 6 is based on the approach of Laakso et al. (2003). However, because of the limitation of available data during the precipitation events, scavenging coefficient in Fig. 6 is from the PM_{10} measurement data. It should be noted that the discrepancy between these results can be from many factors including size region considered. As shown in Fig. 6, both studies showed a similar trend; however, the findings of this study had a lower value than that reported by Laakso et al. (2003).

Table 3 shows the comparisons of the below-cloud scavenging coefficient (Λ_m, hr^{-1}) expressed as aR^b in the current and previous studies. Here, the rainfall rate R was expressed in mm h^{-1}. The coefficients a and b had various ranges depending on conditions, such as location, precipitation period, size distribution, and other physical assumptions.

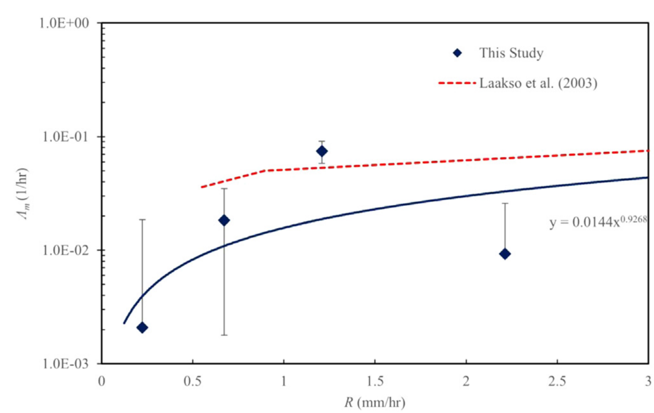

Fig. 6 – Comparison between the obtained and observation-based scavenging coefficient as a function of rain intensity based on Eq. (35).

Fig. 7 shows the comparison of the mass scavenging coefficient as a function of rain intensity for polydisperse size distribution between the present and previous studies. The rain intensity (x-axis) is expressed as log scale in order to investigate wide ranges of rain intensity. The observation and results in the present study with several different size distributions (d_g of 0.3 μm with GSD of 1.5 and d_g of 1.5 μm with GSD of 2.5) were compared with the results in Jylhä (1999), Choi et al. (2020), and GEOS-Chem model parameters (Wang et al., 2011). As shown in Fig. 7, the results of the previous studies showed a large variation. The results in the present study also showed a variation of the mass scavenging coefficient with the size distribution.

In this study, the sensitivity of $PM_{2.5}$ concentrations to different wet scavenging coefficients was tested using a 3D global atmospheric chemical transport model (Geos-Chem). The detailed conditions with description for Geos-Chem simulation are found in the Appendix (Liu et al., 2001; The International GEOS-Chem User Community, 2021). Fig. 8 shows the total precipitation and the $PM_{2.5}$ concentrations during precipitation

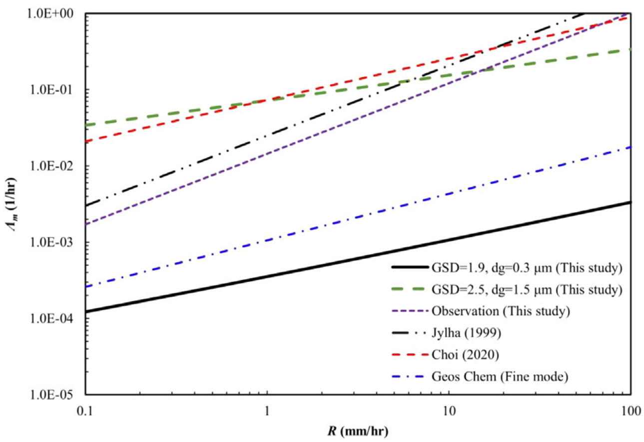

Fig. 7 – Comparison of the mass scavenging coefficients obtained in this study and previous studies as a function of rain intensity for polydisperse size distributions.

events with different scavenging coefficients selected from Table A2. Fig. A3 presents this tendency in East Asia. The scavenging coefficients (Λ_m) of $0.0144R^{0.9268}$ for case 1 (Eq. (33)), $0.0272R^{0.343}$ for case 2, and $0.0724R^{0.3328}$ for case 3 were compared with the default GEOS-Chem coefficient of $0.00106R^{0.61}$. In cases 2 and 3, we tried to show how the change of geometric mean diameter affects the scavenging coefficient at the same GSD. We assume GSD of 2.5 to represent wide distribution case as a single source mode (Horvarth et al., 1990) and d_g of 0.9 and 1.5 μm to represent particle modes change. Since the model uses the assimilated meteorology, the total precipitation obtained from the model and observations were in well agreement. However, the GEOS-Chem default model overestimated the overall $PM_{2.5}$ in South Korea. Table A3 shows the observation sites used in comparison with the GEOS-Chem modeled precipitation and $PM_{2.5}$ for the precipitation event. Thus, when using the derived coefficients, the spatial distribution of $PM_{2.5}$ changes considerably.

As shown in Fig.8, case 3, which uses a coefficient derived for d_g=1.5 μm and GSD = 2.5, reproduces the closest $PM_{2.5}$ to the observations among all cases. The best performing coefficient can vary by region depending on the size distribution of polydisperse aerosols. Therefore, a set of coefficients with ranges for d_g and GSD as proposed in this study can be used for elaborating $PM_{2.5}$ estimation by combining with a module calculating aerosol size distributions (e.g., TOMAS in GEOS-Chem (Lee et al., 2009)) in a 3D CTM.

3. Conclusions

The wet deposition process has an important computational issue. The other removal process, such as dry deposition, is computed only for particles very near the ground. However, wet deposition is computed at all heights (Loosmore and Cederwall, 2004). This computational issue becomes more serious when considering polydisperse aerosols and drop size distribution. Theoretically, the raindrop diameter should be size-resolved to better simulate real settings. When considering polydispersed raindrop size distribution, collection efficiency and scavenging coefficient have a complex functional relation with aerosol size distribution. These complexities increase the computational burden, thereby prolonging numerical calculation.

For these reasons, many 3-D CTMs (e.g., CAMx, Unified Regional Air-Quality Modelling System, etc) apply the monodisperse method scaled by precipitation intensity to calculate the raindrop diameter owing to the computational burden (Wang et al., 2010; Lu and Fung, 2018). These below-cloud

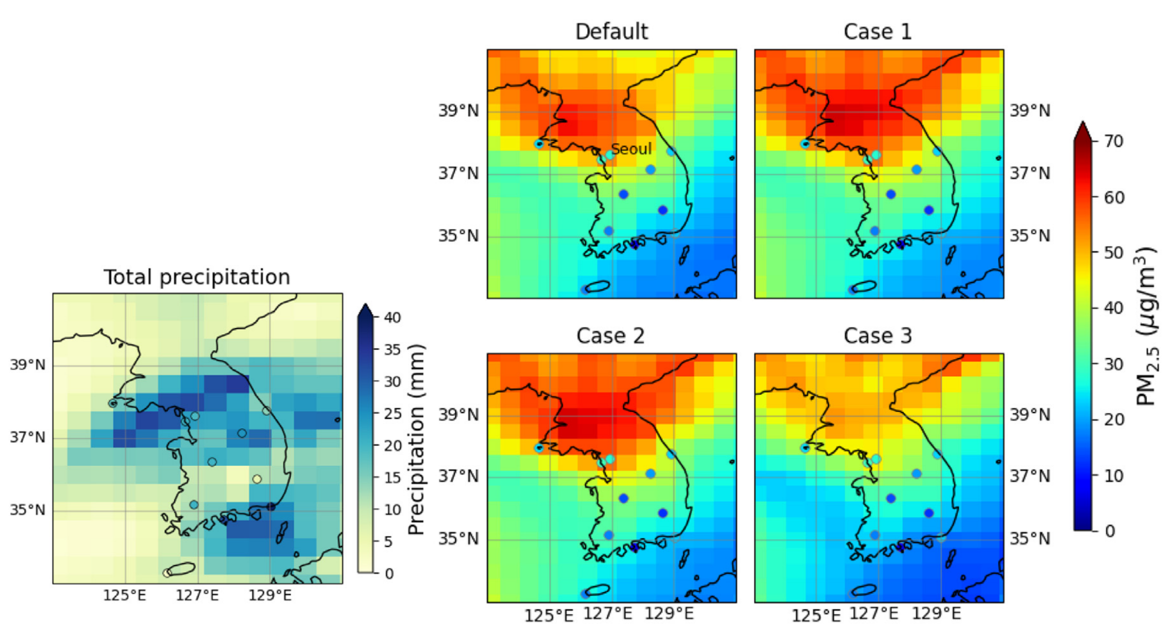

Fig. 8 – Total precipitation during March 20 [6:00 UTC] – 21 [6:00 UTC], 2019 (left), and $PM_{2.5}$ mass concentration averaged over the period (right). Gridded values are GEOS-Chem model output using different scavenging coefficients in Table S2 and circles represent surface observations from Air Korea sites listed in Table S3.

scavenging parameters in large-scale aerosol models is unrealistic owing to the lengthy computational time involved. The estimates of below cloud scavenging in global or chemistry transport models made crude approximations regarding the size distribution of the raindrops or the rainfall rate estimates (Gong et al., 2003; Jacobson, 2003; Loosmore and Cederwall, 2004; Tost et al., 2006; Henzing et al., 2006; Feng, 2007; Berthet et al., 2010; Seinfeld and Pandis, 2016). For these reasons, many studies have described the size-resolved aerosol load as a diagnostic variable and were confined to precipitation-free episodes, so that wet removal can be neglected (Schulz et al., 1998; Collins et al., 2001; Vignati et al., 2001; Henzing et al., 2006).

In this study, we developed an analytic solution for the below-cloud scavenging process of polydisperse fine mode aerosols, including Aitken and accumulation modes, where the diffusion and interception mechanisms were dominant. Based on the collection efficiency determined by Jung and Lee (1998) and the consideration of the C_c factor with simple approximation (Jung et al., 2020), the scavenging coefficient was derived with the M–P raindrop and lognormal aerosol size distributions. Based on the derived analytic solution, we approximated the scavenging coefficient to be a power of the rain intensity for polydisperse aerosols. The parametrized coefficients a and b were expressed as a function of the geometric mean diameter and the GSD of the aerosol size distribution. Here, coefficients a and b for the scavenging coefficient as a power function of rain intensity were derived from the linear regression of the theoretical scavenging coefficients for polydisperse aerosols. The approximated expression obtained was compared with observations in the previous studies. Further, a comparison of the mass concentration during precipitation between the different scavenging coefficients was also conducted using a 3D model simulation.

The resultant expressions from our study are as follows: i) scavenging coefficient at particle diameter Eq. (17)), ii) the number mean (Eq. (25)) and mass mean scavenging coefficient (Eqs. (28) and ((30)) for polydispersed aerosol, and (iii) aerosol size distribution dependent scavenging coefficient as a function of rain intensity (Eqs. (32) and (33)). These newly derived expressions can make the integration of polydisperse raindrops and aerosol size distribution analytically, which consequently reduces computational time in large-scale models. These expressions can also be conveniently compared with observation-based scavenging coefficient by considering polydisperse aerosol size distribution. Comparison showed that the scavenging coefficient could vary according to the size distribution and other factors related to aerosol scavenging. Subsequently, the resulting simple expression can be effectively used to simulate the change in polydispersed aerosol size distribution during precipitation. Though the obtained expression was developed with the M–P raindrop and lognormal aerosol size distributions, as shown, the approach can be applied to different raindrop size distribution.

Becuse of many factors which affect aerosol scavenging during the precipitation, it is still challenging to demonstrate the reliability of this study and generalize the theoretical solutions to spatial-temporally different scavenging cases. In order to show the validity of the solution, a more observational-based comparison with various precipitation cases should be conducted and this has remained for further study.

Acknowledgments

This study was supported by the FRIEND (Fine Particle Research Initiative in East Asia Considering National Differences) Project through the National Research Foundation of Korea (NRF) funded by the Ministry of Science and ICT (No. 2020M3G1A1114617); the Technology Development Program to Solve Climate Changes through the National Research Foundation of Korea (NRF) funded by the Ministry of Science, ICT (No. 2019M1A2A2103953); the National Research Foundation of Korea Grant from the Korean Government (MSIT) (Nos. NRF2021M1A5A1065672/PN22011, NRF2021R1F1A1046878, and NRF2020R1A2C1003215). This research was also supported by Basic Science Research Program through the National Research Foundation of Korea (NRF) funded by the Ministry of Education (No. 2020R1A6A1A03044834).

Supplementary materials

Supplementary material associated with this article can be found, in the online version, at doi:10.1016/j.jes.2022.07.031.

REFERENCES

Allen, M.D., Raabe, O.G., 1985. Slip correction measurements of spherical solid aerosol particles in an improved Millikan apparatus. Aerosol Sci. Technol. 4, 269–286.

Andronache, C., 2003. Estimated variability of below-cloud aerosol removal by rainfall for observed aerosol size distributions. Atmos. Chem. Phys. 3, 131–143.

Andronache, C., 2004. Diffusion and electric charge contributions to below-cloud wet removal of atmospheric ultra-fine aerosol particles. J. Aerosol Sci. 35, 1467–1482.

Bae, S.Y., Jung, C.H., Kim, Y.P., 2006. Development and evaluation of an expression for polydisperse particle scavenging coefficient for the below-cloud scavenging as a function of rain intensity using the moment method. J. Aerosol Sci. 37, 1507–1519.

Bae, S.Y., Jung, C.H., Kim, Y.P., 2010. Derivation and verification of an aerosol dynamics expression for the below-cloud scavenging process using the moment method. J. Aerosol Sci. 41, 266–280.

Baklanov, A., Sørensen, J.H., 2001. Parameterisation of radionuclide deposition in atmospheric long-range transport modelling. Phys. Chem. Earth B 26, 787–799.

Berthet, S., Leriche, M., Pinty, J.P., Cuesta, J., Pigeon, G., 2010. Scavenging of aerosol particles by rain in a cloud resolving model. Atmos. Res. 96 (2–3), 325–336.

Choi, Y., Kanaya, Y., Takigawa, M., Zhu, C., Park, S.-M., Matsuki, A., et al., 2020. Investigation of the wet removal rate of black carbon in East Asia: validation of a below- and in-cloud wet removal scheme in FLEXible PARTicle (FLEXPART) model v10.4. Atmos. Chem. Phys. 20, 13655–13670.

Croft, B., Lohmann, U., Martin, R.V., Stier, P., Wurzler, S., Feichter, J., et al., 2009. Aerosol size-dependent below-cloud scavenging

by rain and snow in the ECHAM5-HAM. Atmos. Chem. Phys. 9, 4653–4675.
Ekerete, K.'u.-M.E., Hunt, F.H., Jeffery, J.L., Otung, I.E., 2015. Modeling rainfall drop size distribution in southern England using a Gaussian mixture model. Radio Sci. 50, 876–885.
Grythe, H., Kristiansen, N.I., Groot Zwaaftink, C.D., Eckhardt, S., Ström, J., Tunved, P., et al., 2017. A new aerosol wet removal scheme for the Lagrangian particle model FLEXPART v10. Geosci. Model Dev. 10, 1447–1466.
Gussman, R.A., 1969. On the aerosol particle slip correction factor. J. Appl. Meteorol. 8 (6), 999–1001.
Henzing, J.S., Olivié, D.J.L., van Velthoven, P.F.J., 2006. A parameterization of size resolved below cloud scavenging of aerosols by rain. Atmos. Chem. Phys. 6, 3363–3375.
Hinds, W.C., 1998. Aerosol Technology, Properties Behavior, and Measurement of Airborne Particles, 2nd ed. John Wiley and Sons, New York.
Horn, H.-G., Bonka, H., Gerhards, E., Hieronimus, B., Kalinowski, M., Kranz, L., et al., 1988. Collection efficiency of aerosol particles by raindrops. J. Aerosol Sci. 19, 855–858.
Horvath, H., Gunter, R.L., Wilkison, S.W., 1990. Determination of the coarse mode of the atmospheric aerosol using data from a forward-scattering spectrometer probe. Aerosol Sci. Technol. 12 (4), 964–980.
Jaenicke, R., 1993. Tropospheric Aerosols, in: Aerosol-Cloud-Climate Interactions. Hobbs, P. Academic Press, San Diego, California, pp. 1–31.
Jung, C.H., Lee, K.W., 1998. Filtration of fine particles by multiple liquid droplet and gas bubble systems. Aerosol Sci. Technol. 29, 389–401.
Jung, C.H., Kim, Y.P., Lee, K.W., 2002. Simulation of the influence of coarse mode particles on the properties of fine mode particles. J. Aerosol Sci. 33, 1201–1216.
Jung, C.H., Kim, Y.P., Lee, K.W., 2003. A moment model for simulating raindrop scavenging of aerosols. J. Aerosol Sci. 34, 1217–1233.
Jung, C.H., Yoon, Y.J., Um, J., Lee, S.S., Lee, J.Y., Chiao, S., et al., 2020. Approximation of most penetrating particle size for fibrous filters considering Cunningham slip correction factor. Environ. Eng. Res. 25, 439–445.
Jylhä, K., 1991. Empirical scavenging coefficients of radioactive substances released from Chernobyl. Atmos. Environ. 25, 263–270.
Jylhä, K., 1999. Relationship between the scavenging coefficient for pollutants in precipitation and the radar reflectivity factor. Part I: derivation. J. Appl. Meteor. 38, 1421–1434.
Kathiravelu, G., Lucke, T., Nichols, P., 2016. Rain drop measurement techniques: a review. Water. 8, 29.
Kessler, E., 1969. On the Distribution and Continuity of Water Substance in Atmospheric Circulations. Meteorol. Monogr. 10.
Laakso, L., Grönholm, Rannika, Ü., Kosmalea, M., Fiedlera, V., Vehkamäki, H., Kulmalaa, M., 2003. Ultrafine particle scavenging coefficients calculated from 6 years field measurements. Atmos. Env. 37, 3605–3613.
Lee, K.W., Liu, B.Y.H., 1980. On the minimum efficiency and the most penetrating particle size for fibrous filters. J. Air Pollut. Control Assoc. 30, 337–381.
Lee, Y.H., Chen, K., Adams, P.J., 2009. Development of a global model of mineral dust aerosol microphysics. Atmos. Chem. Phys. 9, 2441–2458.
Liu, H., Jacob, D.J., Bey, I., Yantosca, R.M., 2001. Constraints from 210Pb and 7Be on wet deposition and transport in a global three-dimensional chemical tracer model driven by assimilated meteorological fields. J. Geophys. Res. 106 (109–112), 128.
Liu, X., Wan, Q., Wang, H., Xiao, H., Zhang, Y., Zheng, T., et al., 2018. Raindrop size distribution parameters retrieved from Guangzhou S-band polarimetric radar observations. J. Meteor. Res. 32 (4), 571–583.
Loosmore, G.A., Cederwall, R.T., 2004. Precipitation scavenging of atmospheric aerosols for emergency response applications: testing an updated model with new real-time data. Atmos. Env. 38, 993–1003.
Luo, G., Yu, F., Moch, J.M., 2020. Further improvement of wet process treatments in GEOS-Chem v12.6.0: impact on global distributions of aerosols and aerosol precursors. Geosci. Model Dev. 13, 2879–2903.
Luo, G., Yu, F., Schwab, J., 2019. Revised treatment of wet scavenging processes dramatically improves GEOS-Chem 12.0.0 simulations of surface nitric acid, nitrate, and ammonium over the United States. Geosci. Model Dev. 12, 3439–3447.
Marshall, J.S., Palmer, W.M.K., 1948. The distribution of raindrops with size. J. Meteor. 5, 165–166.
Okita, T., Hara, H., Fukuzaki, N., 1996. Measurements of atmospheric SO2 and SO42−, and determination of the wet scavenging coefficient of sulfate aerosols for the winter monsoon season over the Sea of Japan. Atmos. Environ. 30, 3733–3739.
Pruppacher, H.R., Klett, J.D., 1978. Microphysics of Clouds and Precipitation. D. Reidel Publishing Company.
Schmid, O., Trueblood, M.B., Gregg, N., Hagen, D.E., Whitefield, P.D., 2002. Sizing of aerosol in gases other than air using a differential mobility analyzer. Aerosol Sci. Technol. 36 (3), 351–360.
Scott, B.C., 1982. Theoretical estimates of the scavenging coefficient for soluble aerosol particles as a function of precipitation type, rate and altitude. Atmos. Environ. 16, 1753–1762.
Seinfeld, J.H., Pandis, S.N., 2016. Atmospheric Chemistry and Physics: From Air Pollution to Climate Change. John Wiley & Sons, Inc., New York.
Slinn, W.G.N., 1983. Precipitation Scavenging. Atmospheric Sciences and Power Production—1979. Division of Biomedical Environmental Research, Department of Energy, Washington District of Columbia.
Sorensen, C.M., Wang, G.M., 2000. Note on the correction for diffusion and drag in the slip regime. Aerosol Sci. Technol. 33, 353–356.
Sparmacher, H., Fülber, K., Bonka, H., 1993. Below-cloud scavenging of aerosol particles: particle-bound radionuclides—experimental. Atmos. Environ. 27, 605–618.
Sperber, K.R., Hameed, S., 1986. Rate of precipitation scavenging of nitrates on central Long Island. J. Geophys. Res. 91 (D11), 11833–11839.
Textor, C., Schulz, M., Guibert, S., Kinne, S., Balkanski, Y., Bauer, S., et al., 2006. Analysis and quantification of the diversities of aerosol life cycles within AeroCom. Atmos. Chem. Phys. 6, 1777–1813.
The International GEOS-Chem User Community, 2021. geoschem/Geos-Chem: GEOS-Chem 13.0.0, Zenodo [Code]. doi:10.5281/zenodo.4618180.
Wang, Q., Jacob, D.J., Fisher, J.A., Mao, J., Leibensperger, E.M., Carouge, C.C., et al., 2011. Sources of carbonaceous aerosols and deposited black carbon in the Arctic in winter–spring: implications for radiative forcing. Atmos. Chem. Phys. 11, 12453–12473.
Wang, X., Zhang, L., Moran, M.D., 2010. Uncertainty assessment of current size-resolved parameterizations for below-cloud particle scavenging by rain. Atmos. Chem. Phys. 10, 5685–5705.
Wang, X., Zhang, L., Moran, M.D., 2014. Development of a new semi-empirical parameterization for below-cloud scavenging of size-resolved aerosol particles by both rain and snow. Geosci. Model Dev. 7, 799–819.

Xu, D., Ge, B., Chen, X., Sun, Y., Cheng, N., Li, M., et al., 2019. Multi-method determination of the below-cloud wet scavenging coefficients of aerosols in Beijing, China. Atmos. Chem. Phys. 19, 15569–15581.
Xu, D.H., Ge, B.Z., Wang, Z.F., Sun, Y.L., Chen, Y., Ji, D.S., et al., 2017. Below-cloud wet scavenging of soluble inorganic ions by rain in Beijing during the summer of 2014. Environ. Pollut. 230, 963–973.
Yamagata, S., Kobayashi, D., Ohta, S., Murao, N., Shiobara, M., Wada, M., et al., 2009. Properties of aerosols and their wet deposition in the arctic spring during ASTAR2004 at Ny-Alesund, Svalbard. Atmos. Chem. Phys. 9, 261–270.